Available online at www.sciencedirect.com
SCIENCE DIRECT®
Journal of Molecular Catalysis A: Chemical 223 (2004) 363–369
JOURNAL OF MOLECULAR CATALYSIS A: CHEMICAL
www.elsevier.com/locate/molcata

Characterization and reactivity of molybdenum oxide catalysts supported on Nb_2O_5–TiO_2

Komandur V.R. Chary*, Kondakindi Rajender Reddy, Chinthala Praveen Kumar, Dhachapally Naresh, Vattikonda Venkat Rao, Gerhard Mestl[1]

Catalysis Division, Indian Institute of Chemical Technology, Hyderabad 500 007, India

Received 18 July 2003; received in revised form 20 January 2004; accepted 28 January 2004
Available online 18 September 2004

Abstract

A series of Mo/Nb_2O_5–TiO_2 catalysts with Mo loadings ranging from 1 to 10 wt.% were prepared and characterized by X-ray diffraction (XRD), pulse oxygen chemisorption, laser Raman spectroscopy (LRS) and temperature-programmed reduction (TPR). XRD patterns indicate the presence of a crystalline MoO_3 phase beyond 7 wt.% Mo on Nb_2O_5–TiO_2. Molybdena is found to be present in a highly dispersed state at lower Mo loadings. Pulse oxygen chemisorption results reveal that the oxygen uptake is found to increase with Mo loading up to 5 wt.% and levels off at higher loadings. Temperature-programmed reductions of H_2 suggest that reduction of the catalysts occurs in two stages. The reducibility of Mo/Nb_2O_5–TiO_2 catalysts decreases with increase of Mo loading on the support. Laser Raman spectra shows that the surface molybdate species are present at low Mo loading (<5% Mo) and crystalline MoO_3 bands are observed from 7 wt.% of Mo and above loadings. The catalytic activity during ammoxidation of toluene increases with molybdena loading up to 5 wt.%, which corresponds to monolayer coverage and remains unchanged at higher Mo loadings. A linear correlation is observed between catalytic activity and oxygen chemisorption sites.

Keywords: Mo/Nb_2O_5–TiO_2 catalysts; XRD; TPR; LRS; Toluene ammoxidation

1. Introduction

Supported molybdenum oxide catalysts are the subject of extensive investigation in the recent past because of their importance in many industrial reactions such as hydrodesulphurization (HDS), selective oxidation, ammoxidation and metathesis of olefins [1–15]. The development in the petroleum refining technology in the last three decades raised hydroprocessing reactions to a high level of economic importance. The catalytic properties of the active molybdenum oxide phase can be influenced by the nature of the support and the dispersion of the active component. Niobium oxides have been reported to increase the catalytic activity and selectivity remarkably with enhancement in catalyst life when a small amount of it was added to a known catalyst. Niobium oxide is known to exhibit a pronounced effect as a support for metal or metal oxide catalysts. The addition of Nb to V_2O_5/TiO_2 was found to improve its low temperature activity [16–19]. A remarkable effect of Nb_2O_5 on Rh as catalyst support was reported regarding its activity and selectivity toward higher hydrocarbons in $CO + H_2$ reaction [20]. The support effect is in the order of $Nb_2O_5 > ZrO_2 > Al_2O_3 > SiO_2 > MgO$. Titania and niobia supported molybdena and vanadia catalysts are reported to be highly active for oxidation/ammoxidation reactions [11,21–29]. The inherent favorable properties of titania and niobia supports can be explored fully by the combination of both supports in a mixed oxide. Okazaki and Okuyama [30] examined the catalytic performance of a group of binary metal oxides for NO reduction with ammonia. They found

* Corresponding author. Tel.: +91 40 271 93162; fax: +91 40 271 60921.
E-mail addresses: kvrchary@iict.ap.nic.in, kvrchary@iict.res.in (K.V.R. Chary).
[1] Nano Scape AG, Frankfurter Ring, D-80809 Munich, Germany.

1381-1169/$ – see front matter © 2004 Elsevier B.V. All rights reserved.
doi:10.1016/j.molcata.2004.01.029

that Nb_2O_5–TiO_2 binary oxide showed good catalytic activity when compared to other binary oxides. Our recent studies [31] also reveal that V_2O_5 supported on Nb_2O_5–TiO_2 are active during the ammoxidation of toluene. Thus, the combined binary oxide Nb_2O_5–TiO_2 has attracted much attention recently as a catalyst and as a support for various applications.

Benzonitrile is used as a precursor for resins and coatings. It is also used as an additive in fuels and fibers. Stobbelaar [32] reported that MoO_3/Al_2O_3 catalysts also have comparable activity with other vanadia supported catalysts in the ammoxidation of toluene. The basic problem in catalytic oxidation is the estimation of the number of active sites on the surface of oxide catalysts. Although this remains a challenge, considerable progress has been made for metals in the determination of the quantity of surface atoms of metals. Simple methods to titrate surface metal centers in oxides would greatly assist in understanding the effect of structure in oxidation reactions.

In the present investigation we report the characterization of MoO_3 supported on Nb_2O_5–TiO_2 catalysts by powder X-ray diffraction, pulse oxygen chemisorption, temperature-programmed reduction of H_2 and laser Raman spectroscopy. We also report the correlation between the dispersion of molybdenum oxide and the catalytic properties during the vapour phase ammoxidation of toluene. The purpose of this work is to estimate the dependence of dispersion of molybdenum oxide supported on Nb_2O_5–TiO_2 as a function of Mo loading and also to identify the changes in structure of the molybdena phase with increased active phase loading.

2. Experimental

2.1. Catalyst preparation

A series of MoO_3/Nb_2O_5–TiO_2 catalysts with Mo loadings ranging from 1 to 10 wt.% of Mo was prepared by impregnation of the Nb_2O_5–TiO_2 with ammonium heptamolybdate solution at pH 8. After impregnation, the catalysts were dried at 383 K for 24 h and subsequently calcined in air at 773 K for 6 h. The Nb_2O_5–TiO_2 support (1:1 wt.%) was prepared in the laboratory according to the procedure described elsewhere [30]. Briefly, the typical procedure involves co-precipitation of niobium (V) oxide hydrate and titanium isopropoxide and neutralization with 28% aqueous ammonia, followed by washing to neutral pH and drying at 383 K for 24 h. The resulting mixed hydroxide was calcined at 773 K for 6 h in air.

2.2. Catalyst characterization

X-ray diffractograms were recorded on Siemens D-5000 diffractometer using graphite filtered Cu Kα radiation.

Oxygen chemisorption was measured by dynamic method on AutoChem 2910 (Micromeritics, USA) instrument. Prior to adsorption measurements, 0.5 g of the samples were reduced in a flow of hydrogen (50 ml/min) at 623 K for 2 h and flushed in the pure He flow (99.999%, 50 ml/min) for 1 h at the same temperature. Oxygen uptakes were determined by injecting pulses of oxygen from a calibrated on-line sampling valve onto a He stream passing over the reduced samples at 623 K. Adsorption was deemed to be complete after at least three successive peaks showed the same area. The specific surface areas of the catalysts were determined by the BET method using nitrogen physisorption at 77 K taking 0.162 nm^2 as cross-sectional area of N_2 molecule.

Temperature-programmed reduction (TPR) experiments were carried out on the same AutoChem 2910 (Micromeritics) instrument, which is used for pulse oxygen chemisorption experiments. Prior to TPR the catalyst sample was pretreated by passing ultra high pure helium (50 ml/min) at 673 K for 2 h. After pretreatment the sample was cooled to room temperature. The carrier gas (5% hydrogen–95% argon) purified through oxy-trap and molecular sieves was allowed to pass over the sample. Temperature was raised from ambient to 1273 K at a heating rate of 5 K/min and the data was recorded simultaneously. The hydrogen consumption values are calculated using GRAMS/32 software. More details concerning TPR are discussed elsewhere [22].

The Raman spectra were recorded with a LabRam spectrometer (DILOR) equipped with a confocal microscope (Olympus) and a He–Ne laser. The slit width was usually set to 200 μm resulting together with the used 1800 grating in a spectral resolution of 2 cm^{-1}. The laser power of the He–Ne laser attached to the LabRam spectrometer was set at 0.14 mW by neutral density filters.

The ammoxidation of toluene to benzonitrile reaction was carried out in a fixed-bed down-flow, reactor with 20 mm internal diameter made of Pyrex glass. An amount of 0.5 g of the catalyst of 18–25 mesh size diluted with an equal amount of quartz grains of the same dimensions was charged into the reactor supported on a glass wool bed. In order to minimize the adverse thermal effects, the catalyst particles were diluted to its same volume with quartz grains of similar particle size. Prior to introducing the reactant toluene with a syringe pump (B-Braun perfusor, Germany) the catalyst was oxidized at 673 K for 2 h in air flow (40 ml/min) and then the reactor was fed with toluene, ammonia and air in the molar ratio of 1:14:30. The zone above the catalyst bed was filled-up with quartz glass particles to serve as the preheater. It is heated up to 423 K for adequate vaporization of liquid feed. The reaction products benzonitrile and benzene were analyzed by HP 6890 gas chromatograph equipped with a Flame Ionization Detector (FID) using HP-5 capillary column. The carbon oxides were analyzed by HP-5973 GC-MS using a carbosieve column.

3. Results and discussion

The X-ray diffraction patterns of calcined MoO_3/Nb_2O_5–TiO_2 catalysts are presented in Fig. 1.

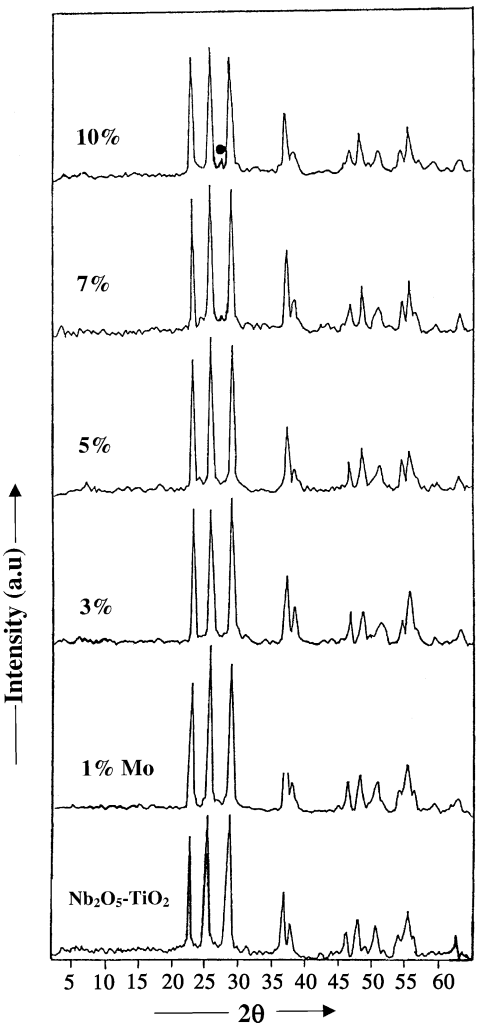

Fig. 1. X-ray diffraction (XRD) patterns of $Mo/Nb_2O_5–TiO_2$ catalysts (●) peak due to MoO_3.

In all the samples XRD peaks due to low temperature niobia were observed at d = 3.95, 3.14, 2.45, 1.97 and 1.66 Å (corresponding 2θ values are 22.5°, 28.4°, 36.6°, 46° and 55.3°, respectively), in addition to anatase titania peaks at d = 3.52, 1.89, 2.37, and 1.48 Å (corresponding 2θ values are 25.3°, 48.1°, 37.8° and 62.7°, respectively). At higher Mo loadings (from 7 wt.% Mo) XRD peak due to crystalline MoO_3 phase is noticed at d = 3.26 Å in addition to the characteristic peaks of niobia and titania. The intensity of this peak increased with molybdena loading. XRD also indicates that no new compound is formed due to the interaction between MoO_3 and TiO_2 or Nb_2O_5. In the present investigation, the $Mo/Nb_2O_5–TiO_2$ samples are calcined at 773 K and XRD results (Fig. 1) suggest the formation of TT-phase of Nb_2O_5, which is in good agreement with the work of Ko and Weissman [33]. The present XRD results are in good agreement with our earlier studies on MoO_3/TiO_2 [21] and MoO_3/ZrO_2 [34] catalysts, wherein crystalline MoO_3 appeared above monolayer coverage.

Table 1
Results of oxygen uptake, dispersion, oxygen atom site density and surface area of $MoO_3/Nb_2O_5–TiO_2$ catalysts

Mo loading (wt.%)	Surface area ($m^2\ g^{-1}$)	Oxygen uptake[a] ($\mu mol\ g^{-1}$)	Oxygen atom site density ($\times 10^{18}\ m^{-2}$)	Dispersion[b] O/Mo
1	55	49.5	0.5	0.92
3	51	140	1.6	0.89
5	49	220	2.7	0.84
7	46	261	3.3	0.71
10	42	312	4.4	0.60

[a] $T_{red} = T_{ads}$ = 623 K.
[b] Dispersion = fraction of Mo atoms at the surface assuming $O_{ads} = Mo_{surf}$ = 1.

The specific surface areas determined by nitrogen physisorption for all catalysts are presented in Table 1. The specific surface area decreases as a function of molybdena content on niobia–titania, which might be due to blocking of the pores of the support by crystallites of molybdena as evidenced by XRD. The oxygen uptake values of various catalysts are presented in Table 1 and the other information such as oxygen atom site density, dispersion, etc., derived from it are also reported in Table 1. The oxygen atom site density, defined as the number of oxygen atoms chemisorbed per unit area of the reduced MoO_3 surface, was found to increase with the increase of Mo loading.

Fig. 2 shows the oxygen uptake of various $Mo/Nb_2O_5–TiO_2$ catalysts measured at 623 K as a function of molybdena content on $Nb_2O_5–TiO_2$. At low Mo loadings the oxygen uptake approaches the straight line corresponding to a stoichiometry of one oxygen atom per molybdenum atom (Table 1). At high Mo loadings the oxygen uptake values are found to deviate from the straight line. The straight line corresponds to a 100% dispersion of the MoO_3 with a stoichiometry of one oxygen atom per molybdenum atom (Fig. 2). The deviation from the straight line beyond

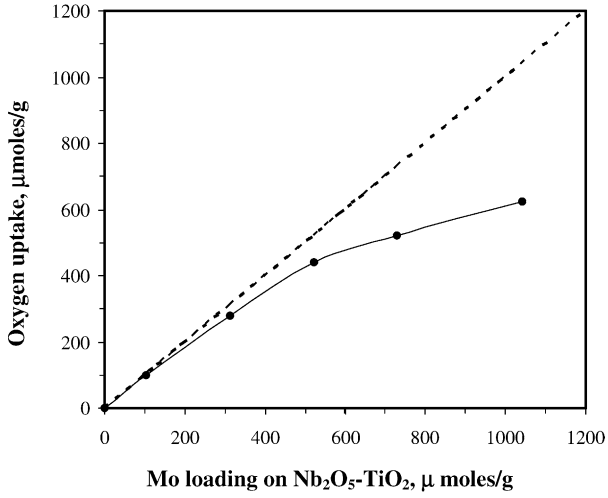

Fig. 2. Oxygen uptake plotted as a function of molybdena loading $T_{ads} = T_{red}$ = 623 K.

Table 2
Results of temperature-programmed reduction of MoO_3/Nb_2O_5–TiO_2 catalysts

Mo content (wt.%)	T^1_{red} (K)	H_2 uptake (ml g^{-1})	T^2_{red} (K)	H_2 uptake (ml g^{-1})	T^3_{red} (K)	H_2 uptake (ml g^{-1})
1	687	0.60	1038	1.6	1143	0.9
3	705	9.90	1039	3.9	1144	0.7
5	731	13.0	1059	4.1	1146	0.6
7	724	20.6	1050	4.8	1156	1.2
10	767	24.5	1070	3.5	1160	1.2

5 wt.% Mo loading over Nb_2O_5–TiO_2 support could be due to the formation of large crystallites of MoO_3. This is in agreement with XRD pattern (Fig. 1). The theoretical monolayer capacity of MoO_3 supported on Nb_2O_5–TiO_2 has been calculated based on the method described by van Hengstum et al. [35] taking 0.16 wt.% of MoO_3 per m^2 of support surface. Accordingly, the theoretical monolayer capacity of MoO_3 supported on niobia–titania employed in the present study having a surface area of 55.4 $m^2\,g^{-1}$ corresponds to 8.8 wt.% MoO_3 or 5.86 wt.% Mo. The XRD results of the present work also support the formation of monolayer and show the presence of MoO_3 crystallites from 7 wt.% Mo and above loadings. This is in good agreement with the theoretical monolayer based on the structure of MoO_3.

The TPR profile of pure MoO_3 is reported elsewhere [34] with our work on MoO_3/ZrO_2 catalysts. The profile shows two major peaks at 1040 and 1270 K and one minor reduction peak at 1070 K. For TPR analysis of unsupported MoO_3, the reduction conditions applied were similar to those applied for supported MoO_3/Nb_2O_5–TiO_2 catalysts. According to Thomas [36] and Arnoldy et al. [37], the reduction of molybdena takes place in two steps

$$MoO_3 \rightarrow MoO_2 \quad (1)$$

$$MoO_2 \rightarrow Mo \quad (2)$$

The sharp peak at 1040 K corresponds to reduction of MoO_3 (first step) and the second peak at 1270 K is associated with the reduction of MoO_2. A minor peak at the edge of the first major peak is observed at 1070 K, which corresponds to Mo_4O_{11} formed by the reduction of MoO_3. Thomas et al. [36] also noticed this peak during TPR of MoO_3 by in situ X-ray diffraction.

Temperature-programmed reduction profiles of the Nb_2O_5–TiO_2 supported molybdenum oxide catalysts are shown in Fig. 3. The reduction temperature (T_{red}) positions and hydrogen consumption values are given in Table 2. TPR profiles of niobia–titania supported molybdena catalysts indicate that molybdena reduces in two stages. The first peak was observed in the temperature region 687–767 K and the second peak was in the 1038–1070 K region. The T_{red} values for these two peaks increases with molybdena loading due to increase of particle size, which lowers the dispersion. Oxygen chemisorption results further support these findings. The low

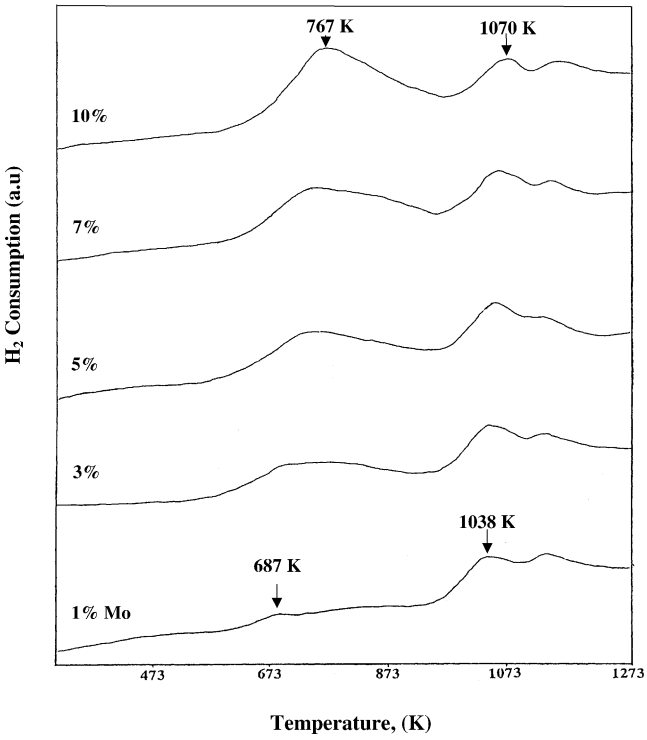

Fig. 3. Temperature-programmed reduction profiles of various Mo/Nb_2O_5–TiO_2 catalysts.

temperature peak is assigned to reduction of molybdenum oxide present in octahedral species and the high temperature peak is assigned to reduction of tetrahedral molybdenum oxide species. The increase in T_{red} values indicates that the interaction of octahedral and tetrahedral molybdena species with the support increases with increase of Mo loading. The third peak in the region (1140–1160 K) of TPR profiles is due to the reduction of Nb_2O_5 [22]. It is well known that niobium oxide is partially reducible when exposed to hydrogen at higher temperatures and the reduction is accelerated by the presence of supported zerovalent metals on its surface [38,39]. The reduction of pure Nb_2O_5 occurs at around 1273 K. However, the reducibility of Nb_2O_5 becomes easier when it is associated with MoO_3, and this can be seen from Fig. 3. It has been observed that the supported molybdenum oxide catalysts reduce at much lower temperature than bulk molybdenum oxide and the reducibility of molybdena is strongly influenced by the kind of support used. The advantage of addition of TiO_2 to Nb_2O_5 is the enhanced the reducibility of molybdena catalysts, i.e. the reducibility of Mo/Nb–Ti catalysts is more than that of Mo/Nb catalysts [40].

Wachs et al. [41] examined supported MoO_3 on different supports, including Nb_2O_5 by laser Raman spectroscopy under in situ and ambient conditions. In situ Raman bands for Mo=O terminal stretching modes are observed at 990 cm^{-1} for the MoO_3 supported on Nb_2O_5. Due to attaining of fairly constant Mo=O frequencies, Wachs et al. [41] concluded that the molecular surface metal oxide structures are inde-

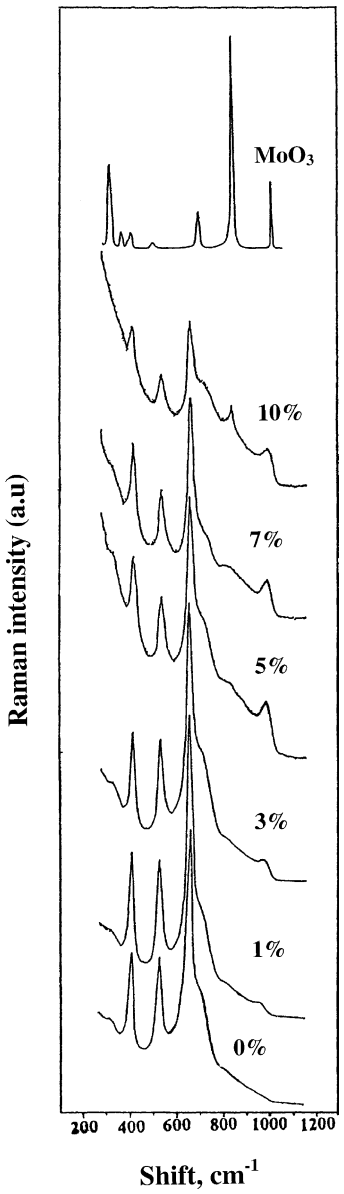

Fig. 4. Laser Raman spectra of $Mo/Nb_2O_5–TiO_2$ catalysts.

pendent of the specific oxide support. Jehng et al. [42] assigned the band at 960 cm^{-1}, observed in Raman spectra of 1–10 wt.% MoO_3/Nb_2O_5 catalysts under ambient conditions, to $Mo_8O_{26}^{4-}$. Kim et al. [43] also studied the Mo/TiO_2 catalysts by laser Raman spectroscopy prepared by equilibrium adsorption method. They observed Raman bands in calcined samples species in the region of 949–958 cm^{-1} due to polymolybdate species, $Mo_7O_{24}^{6-}$ and/or $Mo_8O_{26}^{4-}$. In the present investigation we have studied the Raman spectra of $Mo/Nb_2O_5–TiO_2$ samples under hydrated conditions as shown in Fig. 4. The spectra exhibited a band at 951 cm^{-1}, which is shifted to 975 cm^{-1} with the increase in Mo loading from 1 to 10 wt.% Mo and was assigned to terminal Mo=O stretching mode of hepta- and octamolybdates. The bands due to crystalline MoO_3 are observed from 7 wt.% of Mo loading at 820 cm^{-1}. Hu et al. [44] also observed the crystalline MoO_3 bands at 820 cm^{-1} in Mo/Nb_2O_5 catalysts by laser Raman spectroscopy. According to theoretical monolayer coverage on $Nb_2O_5–TiO_2$ support (surface area: 55.4 $m^2\,g^{-1}$) the MoO_3 required to form monolayer is 8.8 wt.% of MoO_3 or 5.9 wt.% of Mo are required on $Nb_2O_5–TiO_2$ support. Raman bands due to MoO_3 also appeared at 7 wt.% Mo and above loadings, which is in good agreement with the theoretical calculations.

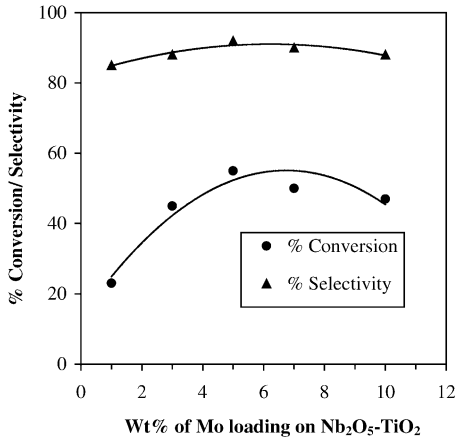

Fig. 5. Ammoxidation of toluene over various $Mo/Nb_2O_5–TiO_2$ catalysts (reaction temperature 673 K).

The catalytic properties evaluated during the vapour phase ammoxidation of toluene for various $MoO_3/Nb_2O_5–TiO_2$ catalysts at 673 K are shown in Fig. 5. The conversion of toluene is found to increase with Mo loading up to 5 wt.% and decreased at higher loadings. However, the selectivity towards benzonitrile formation did not change appreciably with molybdena loading. The activity of the pure $Nb_2O_5–TiO_2$ support was found to be 2% and the activities of the supported catalysts were corrected for support contribution. The activity of $Mo/Nb_2O_5–TiO_2$ was found to be more than that of the Mo/Nb_2O_5 catalysts [29] and comparable with Mo/TiO_2 catalysts [21]. To find the relation between the ammoxidation activity and the dispersion of molybdena, a plot of turn over frequency (TOF, turn over frequency, which is defined as number of toluene molecules converted per second per Mo site) versus the surface molybdena content is shown in Fig. 6. A linear dependence passing through origin was observed, which clearly demonstrates that toluene conversion is directly related to oxygen chemisorption. Oxygen is chemisorbed at low temperatures selectively on coordinatively unsaturated sites (CUS), generated upon reduction, having a particular coordination environment. These sites are located on a highly dispersed molybdena phase, which is formed only at low molybdena loadings and remain as a patchy monolayer on the support surface. At higher Mo loadings, a second phase is formed on the already existing monolayer and this post-monolayer phase does not appreciably chemisorb oxygen. Our studies indicate that the catalytic functionality of the dispersed molybdena phase supported on $Nb_2O_5–TiO_2$ re-

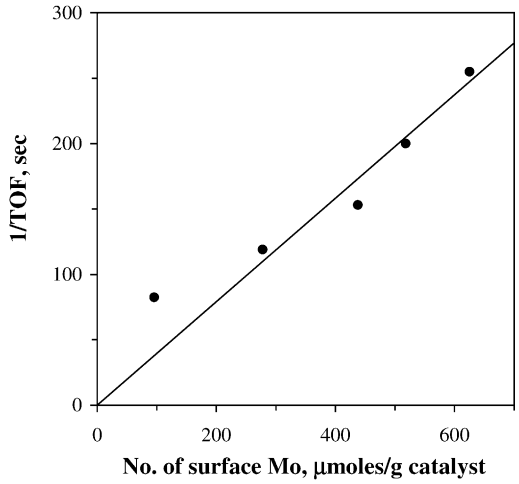

Fig. 6. The relation between turn over frequency (TOF) and surface molybdena atoms.

sponsible for the ammoxidation of toluene to benzonitrile is located on a patchy monolayer phase and this functionality can be titrated by oxygen chemisorption method.

4. Conclusions

Titania modified Nb_2O_5 is found to be an interesting binary oxide support for molybdena. The activity of Mo/Nb_2O_5–TiO_2 was found to more than the Mo/Nb_2O_5 catalysts and comparable with Mo/TiO_2 catalysts. The results of pulse oxygen chemisorption suggest that the molybdena is highly dispersed at lower loadings on Nb_2O_5–TiO_2 support. X-ray diffraction patterns also indicated that molybdena is in highly dispersed state at lower loadings and the reflections due to MoO_3 can be seen only above 5 wt.% of Mo loading. TPR results suggested that the reducibility of MoO_3 decreases with increase of molybdena loading and the reduction of MoO_3 became easier when supported on Nb_2O_5–TiO_2 compared to unsupported MoO_3. Laser Raman spectra showed the bands due to MoO_3 at higher Mo loadings, which are further supported by XRD and pulse oxygen chemisorption results. The catalytic activity during ammoxidation of toluene is correlated with dispersion of molybdena.

Acknowledgements

CBMM, Brazil is gratefully acknowledged for providing gift sample of niobium oxide hydrate. KRR and CHPK are thankful to the Council of Scientific and Industrial Research (CSIR) for the Senior Research Fellowship (SRF) awards.

References

[1] F.E. Massoth, Adv. Catal. 27 (1978) 265.
[2] P. Grange, Catal. Rev.-Sci. Eng. 21 (1980) 135.
[3] H. Knozinger, Proceedings of the Ninth International Congress on Catalysis, Calgary, 1988, M. Phillips, M. Ternan (Eds.), The Chemical Institute of Canada, Ottawa, vol. 5, 1989, p. 20.
[4] B.M. Reddy, K.V.R. Chary, V.S. Subrahmanyam, N.K. Nag, J. Chem. Soc., Faraday Trans. I 81 (1985) 1655.
[5] K.Y.S. Ng, E. Gulari, J. Catal. 95 (1985) 33.
[6] J.S. Chung, R. Miranda, C.O. Bennett, J. Catal. 144 (1988) 898.
[7] C. Louis, J.M. Tatibouet, M. Che, J. Catal. 109 (1988) 354.
[8] Y.C. Liu, G.L. Griffin, S.S. Chan, I.E. Wachs, J. Catal. 94 (1985) 108.
[9] Y. Masuoka, M. Niwa, Y. Murakami, J. Phys. Chem. 94 (1990) 1477.
[10] W. Zhang, A.N. Desikan, S.T. Oyama, J. Phys. Chem. 99 (1995) 14468.
[11] K.V.R. Chary, V.V. Kumar, P. Kanta Rao, Langmuir 6 (1990) 1549.
[12] A.N. Desikan, W. Zhang, S.T. Oyama, J. Catal. 157 (1995) 740.
[13] H. Miyata, T. Mukai, T. Ono, Y. Kubokawa, J. Chem. Soc., Faraday Trans. I 84 (1988) 4137.
[14] I. Matsuura, H. Oda, K. Hoshida, Catal. Today 16 (1993) 547.
[15] R.B. Quincy, M. Houalla, A. Proctor, D.M. Hercules, J. Phys. Chem. 94 (1990) 1520.
[16] F. Kurosawa, Japan Patent Kokai 54-52692 (1979).
[17] H. Utsunomiya, K. Soga, K. Shimazaki, Y. Mito, M. Aoki, S. Haseba, H. Miki, M. Masaki, Ger. Offen 2634279 (1976).
[18] H. Utsunomiya, K. Shimazaki, K. Soga, Y. Mito, M. Aoki, Japan Patent Kokai 52-151688 (1977).
[19] S. Haseba, S. Ito, Y. Mito, T. Hirano, Japan Patent Kokai 55-28718 (1980).
[20] T. Iizuka, Y. Tanaka, K. Tanabe, J. Mol. Catal. 17 (1982) 381.
[21] K.V.R. Chary, K. Rajender Reddy, Ch. Praveen Kumar, Catal. Commun. 2 (2001) 277.
[22] K.V.R. Chary, T. Bhaskar, G. Kishan, K. Rajender Reddy, J. Phys. Chem. 105 (2001) 4392.
[23] K.V.R. Chary, T. Bhaskar, K. Kalyana Seela, K. Srilakshmi, K. Rajender Reddy, Appl. Catal. A: Gen. 208 (2001) 291.
[24] K.V.R. Chary, T. Bhaskar, G. Kishan, V. Vijaykumar, J. Phys. Chem. 102 (1998) 3936.
[25] K.V.R. Chary, G. Kishan, T. Bhaskar, JCS Chem. Commun. (1999) 1399.
[26] K.V.R. Chary, G. Kishan, Ch. Praveen Kumar, G. Vidya Sagar, J.W. Niemantsverdriet, Appl. Catal. A: Gen. 245 (2003) 303.
[27] K.V.R. Chary, G. Kishan, T. Bhaskar, Ch. Sivaraj, J. Phys. Chem. 102 (1998) 6792.
[28] K.V.R. Chary, G. Kishan, K. Srilakshmi, K. Ramesh, Langmuir 16 (2000) 7692.
[29] K.V.R. Chary, K. Rajender Reddy, T. Bhaskar, G. Vidya Sagar, Green Chem. 4 (2002) 206.
[30] S. Okazaki, T. Okuyama, Bull. Chem. Soc. Jpn. 56 (1983) 2159.
[31] Ch. Praveen Kumar, K. Rajender Reddy, V. Venkat Rao, K.V.R. Chary, Green Chem. 4 (2002) 513–516.
[32] P.J. Stobbelaar, Ph.D. Thesis, Technical University of Eindhoven, 2000.
[33] E.I. Ko, J.G. Weissman, Catal. Today 8 (1990) 27.
[34] T. Bhaskar, K. Rajender Reddy, Ch. Praveen Kumar, M.R.V.S. Murthy, K.V.R. Chary, Appl. Catal. A: Gen. 211 (2001) 189.
[35] A.J. van Hengstum, J.G. Van Ommen, H. Bosch, P.J. Gellings, Appl. Catal. 5 (1983) 207.
[36] R. Thomas, Ph.D. Thesis, University of Amsterdam, 1981.
[37] P. Arnoldy, J.C.M. de Jonge, J.A. Moulijn, J. Phys. Chem. 89 (1985) 4517.
[38] S.J. Tauster, S.C. Fung, J. Catal. 55 (1979) 29.
[39] G. Sankar, S. Vasudevan, C.N.R. Rao, J. Phys. Chem. 92 (1988) 1878.

[40] K.V.R. Chary, T. Bhaskar, G. Kishan, K. Rajender Reddy, J. Phys. Chem. B 105 (2001) 4392.
[41] I.E. Wachs, G. Deo, D.S. Kim, M.A. Vuurman, H. Hu, in: L. Guczi, F. Solymosi, P. Tetenyi (Eds.), Proceedings of the 10th International Congress Catalysis, 1992, p. 543.
[42] J.M. Jehng, A.M. Turek, I.E. Wachs, Appl. Catal. A: Gen. 83 (1992) 179.
[43] D.S. Kim, K. Segawa, T. Soeya, I.E. Wachs, J. Catal. 136 (1992) 539.
[44] H. Hu, I.E. Wachs, S.R. Bare, J. Phys. Chem. 99 (1995) 10897.